IEEE Photonics Journal
An IEEE Photonics Society Publication

Open Access

Full-Duplex Self-Recovery Optical Fibre Transport System Based on a Passive Single-Line Bidirectional Optical Add/Drop Multiplexer

Volume 12, Number 5, October 2020

Chung-Yi Li
Ching-Hung Chang, *Member, IEEE*
Dong-Yi Lu

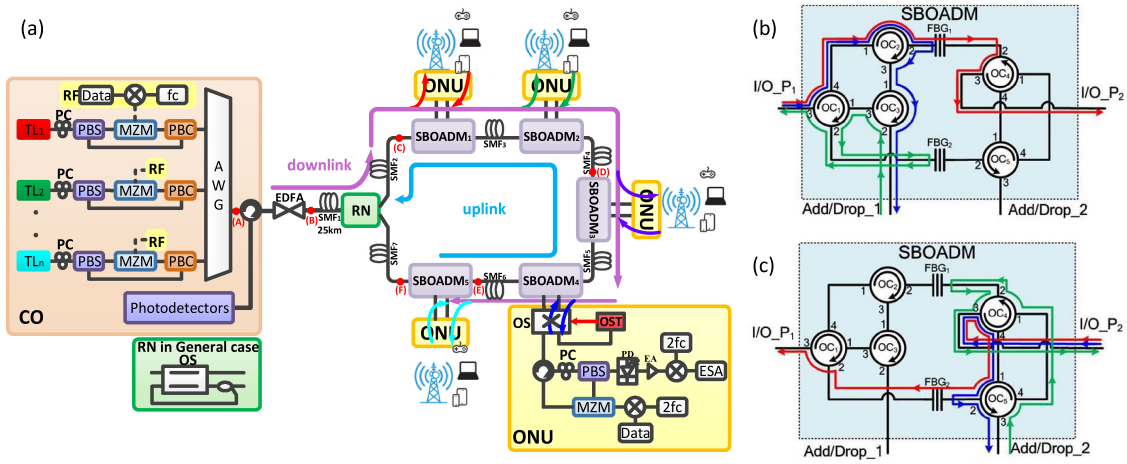

DOI: 10.1109/JPHOT.2020.3022703

IEEE photonics SOCIETY

IEEE

Full-Duplex Self-Recovery Optical Fibre Transport System Based on a Passive Single-Line Bidirectional Optical Add/Drop Multiplexer

Chung-Yi Li,[1] Ching-Hung Chang,[2] *Member, IEEE*, and Dong-Yi Lu[2]

[1]Department of Communication Engineering, National Taipei University, New Taipei City 23741, Taiwan
[2]Department of Electrical Engineering, National Chiayi University, Chiayi 60004, Taiwan

DOI:10.1109/JPHOT.2020.3022703

Manuscript received June 21, 2020; revised August 24, 2020; accepted September 4, 2020. Date of publication September 8, 2020; date of current version October 1, 2020. This work was supported in part by the Ministry of Science and Technology (MOST) of Taiwan under Grants MOST 107-2221-E-415-009-, MOST 108-2221-E-415-023-, and MOST 109-2636-E-305-003- and in part by the University System of Taipei Joint Research Program under USTP-NTUT-NTPU-109-01 Corresponding author: Ching-Hung Chang (e-mail: chchang@mail.ncyu.edu.tw).

Abstract: A full-duplex self-recovery optical fibre transport system is proposed on the basis of a novel passive single-line bidirectional optical add/drop multiplexer (SBOADM). This system aims to achieve an access network with low complexity and network protection capability. Polarisation division multiplexing technique, optical double-frequency application and wavelength reuse method are also employed in the transport system to improve wavelength utilisation efficiency and achieve colourless optical network unit. When the network comprises a hybrid tree–ring topology, the downstream signals can be bidirectionally transmitted and the upstream signals can continuously be sent back to the central office in the reverse pathways due to the remarkable routing function of the SBOADM. Thus, no complicated optical multiplexer/de-multiplexer components or massive optical switches are required in the transport system. If a fibre link failure occurs in the ring topology, then the blocked network connections can be recovered by switching only a single optical switch preinstalled in the remote node. Simulation results show that the proposed architecture can recover the network function effectively and provide identical transmission performance to overcome the impact of a breakpoint in the network. The proposed transport system presents remarkable flexibility and convenience in expandability and breakpoint self-recovery.

Index Terms: Optical add/drop multiplexer, self-healing, wavelength reuse, radio over fiber.

1. Introduction

Under the rapid development of various industry and multimedia applications, a broadband network is an essential tool for emerging artificial Internet of thing applications, intelligent houses/offices/factories and smart sensing and detection systems [1]. Hence, the scope of constructing a fibre optical network system with improved structure reliability whilst simplifying the features for easy operation, maintenance and cost reduction has become increasingly complicated and challenging [2], [3]. An additional standby optical fibre link with an optical switch (OS) must be deployed to prevent network interruption due to the breakdown of optical fibres in traditional

optical fibre access networks, such as time-division multiplexing (TDM) [3]–[6] or wavelength division multiplexing (WDM) [7]–[12] systems. However, such configuration increases the costs of network construction and complicates the network operation. Hence, the bidirectional optical add/drop multiplexer (BOADM) has been developed for the protection of optical fibre networks. The first type of BOADM structure includes the basic optical add/drop multiplexers (OADM) and OSs [13], [14]. Such BOADM can achieve bidirectional transmission in a ring topology optical network. However, the uplink and downlink signals are still transmitted in a fixed direction during the transmission process. The constructed fibre optical networks require the assistance of a backup fibre link to overcome the impact of fibre link failure and additional optical amplifier to compensate for the power loss. To reduce the overall construction cost by taking off backup fibre link, some researchers develop single-wire BOADMs based on OSs, multiplexers and de-multiplexers [15]. Thus, the overall network construction cost can be markedly reduced by utilising the second type BOADMs. The drawback of such BOADM is that its multiplexers and de-multiplexers increase the overall insertion loss in the fibre optical networks. Moreover, the network manager needs a complicated strategy to manage the status of OSs inside each BOADM to reset the routeing pathway of data transmission dynamically during fibre link failure in the network.

Reducing the cost in network usage will be one of the key issues to increase the willingness of customers to say yes to promote the population of fibre optical networks. One of the remarkable costs for a traditional WDM fibre optical network system is the specific light source for uplink transmission established in each optical network unit (ONU). Unlike the central office (CO) end, the hardware cost in each ONU has no sharing capability. Configuring specific light sources in each ONU increases the cost of network usage and results in storage problems of various laser diodes with different wavelengths. Therefore, configuring colourless ONU modules has been a major research direction in current WDM related techniques [16]–[18]. Today, many different kinds of colourless ONU modules, such as the wavelength reutilisation using amplitude modulation, phase to amplitude modulation and reflective semiconductor optical amplifier, have been proposed [19]–[22]. However, these methods require complex modulation skills for reducing the impact of downlink signals on uplink signals.

A full-duplex self-recovery optical fibre transport system for broadband wireless network is proposed in this paper to realise high reliability based on a novel passive single-line BOADM (SBOADM) and colourless ONUs. The SBOADM is originally proposed to achieve the feature of bidirectional transmission in fibre sensor networks [23]. Single-line bidirectional transmission can be easily achieved by the SBOADM without the assistance of a power supply and OS by flexibly employing two fibre Bragg gratings (FBGs) and five optical circulators (OCs) to compose the SBOADM. When the SBOAMD is deployed in a ring topology, an extra logical optical passage is embedded for the network without utilising a backup fibre link. The SBOADM can automatically send the uplink signal back to the CO end along the revised pathway of the downlink signal as long as the downlink signal can be sent smoothly to each ONU end. No additional power supply and complexity control algorithm are required during the entire transmission process. Furthermore, the polarisation division multiplexing (PDM) technique is employed in the proposed system to achieve colourless ONU. When an optical signal with a specific wavelength is captured to a specific ONU, the central carrier wave of the optical signal is withdrawn by a polarised light splitter and reused to deliver upstream signals back to the CO end. Depending on the research discussed by Z. Jia et al., the penalty of utilizing the same wavelength for both downlink and uplink transmission is not significant [24]. Such a structure improves the usage efficiency of the frequency spectrum and reduces the network cost of each ONU end.

2. Experimental Setup

The experimental configuration of the proposed full-duplex self-recovery optical fibre transport system is plotted in Fig. 1(a). At the CO side, each downstream optical carrier is generated by a distributing feedback laser diode (DFB LD), and its power is split into two equal parts via a polarisation beam splitter (PBS). One part of the carrier is directly sent to a polarisation

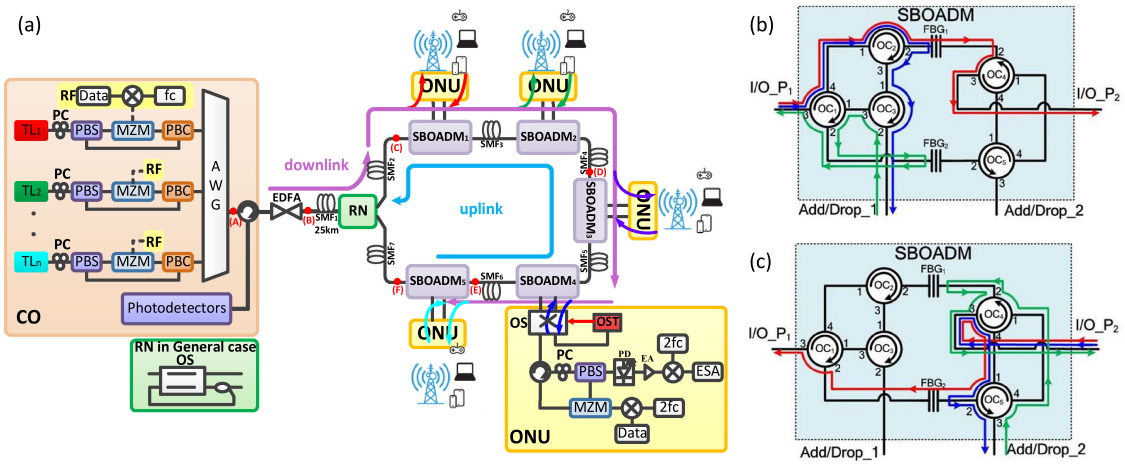

Fig. 1. (a) Configuration of the proposed full-duplex self-recovery optical fibre transport system based on a passive single-line bidirectional optical add/drop multiplexer. (b) The configuration of the proposed passive SBOADM and optical pathways when signals are fed in I/O_P_1 and (c) I/O_P_2.

beam coupler (PBC), and another part is modulated to downstream 3 Gbps/10 GHz signal via Mach–Zender modulator (MZM). The central carrier is suppressed by biasing the MZM at the minimum transmission point to leave only ± 1 side bands on the MZM output. Next, the MZM output signal is directed to the PBC to form a downstream optical signal for an ONU. Consequently, each downstream optical signal is coupled through an arrayed-waveguide grating and amplified by an Erbium-doped optical fibre amplifier (EDFA) before sending to remote nodes (RNs) via a 25 km single-mode fibre1 (SMF1). A 2×2 OS and a 1×2 optical coupler are employed inside the RN to direct the combined downstream signals to each SBOADM via clockwise or ant-clockwise direction. The RN and five SBOADMs are bridged in ring topology by SMF2–SMF7, which are set as 1 km in each, to simulate the metropolitan environment. The OS inside the RN is normally set in parallel status such that the downstream signals can be directed to SBOADM1–SBOADM5 via clockwise direction. As shown in Fig. 1(b), The SBOADM consists of three four-port OCs, two three-port OCs and two identical FBGs with reflection rate of 99%. When optical signals are inputted into the main network via I/O_P1, the signals are directed to FBG1 after passing OC1 and OC2. Subsequently, the FBG1 will reflected back the targeted signals and directed to Add/Drop_1 after passing OC2 and OC3 (blue path in Fig. 1(b), whereas the other optical wavelengths will pass through FBG1 and return to the main network via OC4 to I/O_P2 (red path in Fig. 1(b). When the connected ONU needs to uplink optical signals, the uplink optical signal goes to FBG2 via OC3 and OC1. At the moment, the uplink and downlink optical signals use the same wavelength. As FBG2 has the same characteristics as FBG1, the uplink optical signal is reflected back to OC1 and returns to I/O_P1 (green path in Fig. 1b). Similarly, Fig. 1(c) shows that when optical signal is inputted into the main network via I/O_P2, the signal is directed from OC4 to OC5 and from OC5 to FBG2. The target wavelength is then reflected back by FBG2, goes through OC5 to Add/Drop_2 (blue path in Fig. 1c), whereas the other optical wavelengths will pass through FBG2 and return to the main network via OC1 to I/O_P1 (red path in Fig. 1c). Meanwhile, the uplink optical signal goes to FBG1 via OC5 and OC4. As the uplink and downlink optical signals use the same wavelength, the uplink optical signal is reflected back to OC4 and returns to I/O_P2 (green path in Fig. 1c). Whatever the optical signals are fed into the SBOADM via I/O_P1 or I/O_P2, a 2×2 OS and an optical switch trigger (OST) inserted in each ONU are utilised to bridge the SBOADM two add/drop ports with the connected ONU transceiver circuit. The OST is a simple optical receiver model that can output a high-voltage pulse to change the 2×2 OS status when receiving optical signals. The 2×2 OS is originally in a cross status; therefore, the dropped signal can be directed to the receiver circuit directly. The central

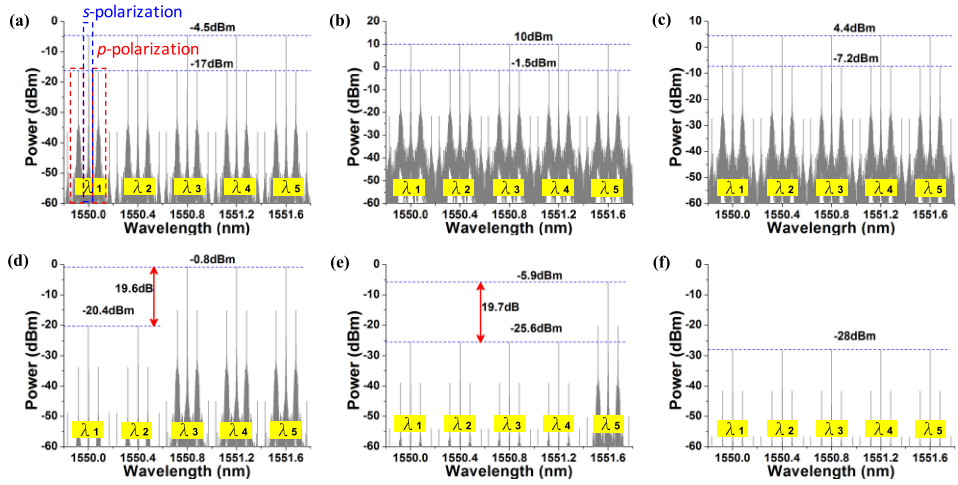

Fig. 2. Spectra derived from the simulation considering the observation points (A)–(F) in Fig. 1(a).

carrier and the ±1 side bands of the downstream signal in the ONU are then separated by a PBS. The signals of ±1 side bands are transformed into 3 Gbps/20 GHz signals via a photodetector (PD), whereas the separated central carrier is reused to modulate with 3 Gbps/10 GHz uplink signal via MZM and send back signals to CO along the reverse downstream transmission pathway. The MZM in the ONU is biased at the peak transmission point to reduce interference amongst downstream and upstream transmissions. The ±1 side bands are suppressed to leave only the central carrier and ±2 side bands at the MZM output. The bandwidth requirement of the MZMs and other electrical circuits in the CO can be significantly reduced because the frequency of the transmitted signals is doubled in the optical domain.

3. Simulation Results and Discussion

A commercial software, namely, VPI Transmission Maker, was employed to facilitate the systematic simulation and verification to prove the feasibility of the proposed full-duplex self-recovery optical fibre transport system. Fig. 2(a) to (f) show the spectra derived from the simulation considering the observation points (A) to (F) in Fig. 1(a). Fig. 2(a) shows the simulated output spectra of five downstream optical signals, with central wavelengths of 1550.0 (λ1), 1550.4 (λ2), 1550.8 (λ3), 1551.2 (λ4) and 1551.6 nm (λ5). The optical power of the spectrum is approximately −4.5 dBm at the central wavelength, whereas that of the ±1 optical side bands are approximately −17 dBm. Fig. 2(b) shows the output spectrum after amplification by the EDFA whose optical power is approximately 10 dBm at the central wavelength, whereas that of the ±1 optical side wave bands is approximately −1.5 dBm. After transmission over 25 km SMF1, RN and 1 km SMF2, the central wavelength and side band power of each downstream signal are roughly 4.4 and −7.2 dBm, respectively, as shown in Fig. 2(c). Fig. 2(d) shows the spectrum of optical signals passing through SBOADM1 and SBOADM2. The λ1 and λ2 can still be observed because the FBGs employed in each SBOADM are imperfect. The central wavelength power of signals with and without be dropped by the SBOADM1 and SBOAMD2 is approximately −20.4 and −0.8 dBm, respectively. Fig. 2(e) shows the spectrum of the optical signals passing through the SBOADM4. The central wavelength power of signals with and without be dropped by previous SBOADMs is approximately −25.6 dBm −5.9 dBm, respectively. These values are roughly 5.2 and 5.1 dB smaller than that shown in Fig. 2(d). However, the relative power division amongst the dropped and passed signals is roughly the same (19.6 versus 19.7 dB). Fig. 2(f) shows the spectrum of the downstream optical signals passing through all SBOADM nodes. The optical power of all

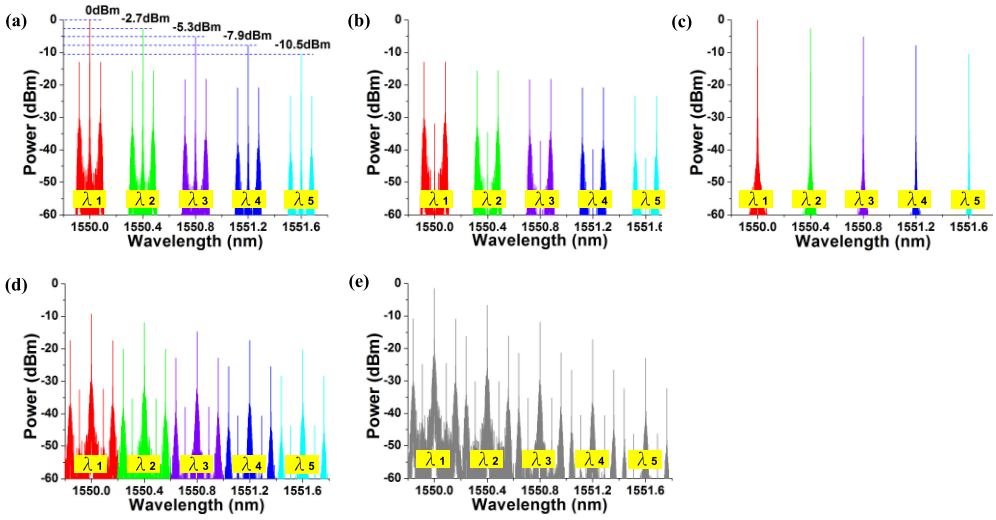

Fig. 3. Spectrum chart. (a) downstream signal dropped by each SBOADM; (b) ± 1 order side band of downstream signals separated by the PBS in each ONU; (c) central carrier of downstream signals separated by the PBS in each ONU; (d) re-modulated uplink optical signal at each ONU; and (e) uplink optical signal received at the CO end.

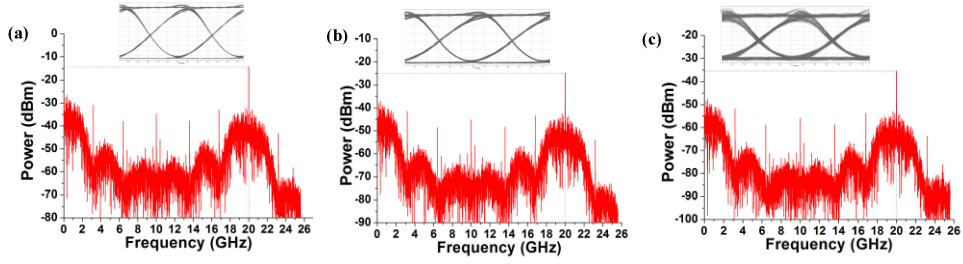

Fig. 4. Electric frequency spectrum and eye diagram of downstream signal measured at (a) ONU1, (b) ONU3, and (c) ONU5.

wavelengths is approximately -28 dBm. These remaining optical signals will be fed into the RN via the SMF7 and then automatically eliminated when passing through an infinite loop of 2×1 optical coupler and OS inside the RN.

The spectra of the downstream optical signals dropped by each SBOADM are overlapped and shown in Fig. 3(a). When each dedicated downstream signal is dropped by SBOADM, this signal will be directed to the connected ONU receiver circuit via a cross-status OS and an OC. The central carrier wave of the downstream signal is separated from the ± 1 optical side wave bands through a PBS. Figs. 3(b) and (c) show the overlapped spectra of central carrier wave and ± 1 optical side wave bands separated at each ONU. When the ± 1 optical side wave bands are converted to 3 Gbps/20 GHz RF signal by a PD, the electrical spectra and eye diagrams of the obtained RF signals in the ONU1, ONU3 and ONU5 are shown in Figs. 4(a)–(c). In a random birefringence of buried optical fiber, the propagating signals may typically cause $2 \sim 10^{\circ}$ polarization angles fluctuation and such polarization fluctuations can be compensated by a dynamic polarization control [25]. Each RF signal is observed in 20 GHz range, that is, the frequency of the downstream signals is successfully up-converted. The signal quality is ensured by open and clear eye diagrams. Similarly, the central carrier wave of each downstream signal is reused for upstream transmissions. The optical spectra of the upstream signal observed at each ONU and the CO receiver end are overlapped and

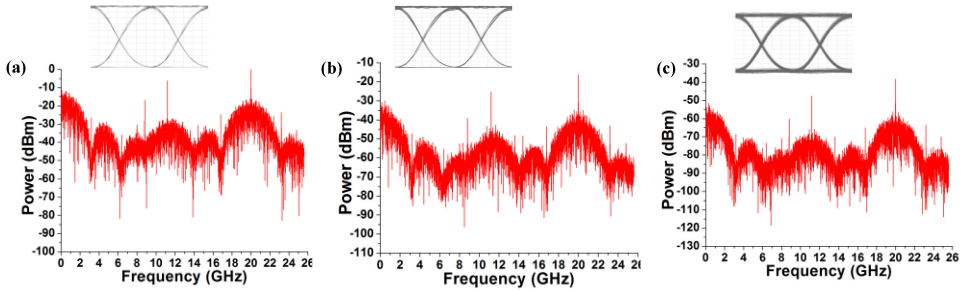

Fig. 5. Electric frequency spectrum and eye diagram of upstream (a) ONU1 signal, (b) ONU3 signal, and (c) ONU5 signal measured at the CO end.

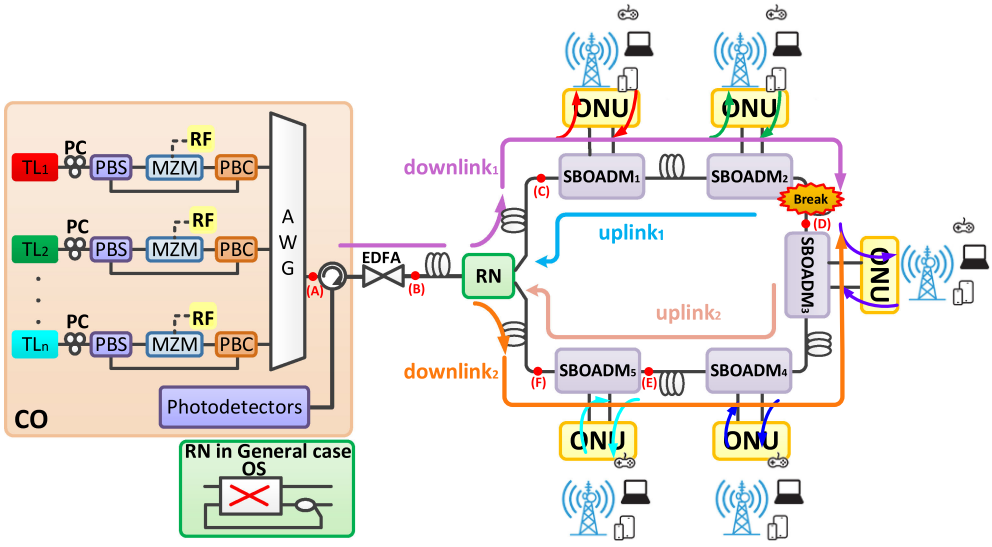

Fig. 6. Schematic of the proposed transport system when a breakpoint occurs between the SBOADM2 and SBOADM3.

presented in Figs. 3(d) and (e), respectively. The upstream signals from the ONU1, ONU3 and ONU5 are still received at the CO end despite the large power deviations amongst the upstream signals, and each upstream 3 Gbps/10 GHz RF signal is properly up-converted to 3 Gbps/20 GHz. The signal transmission quality is ensured by the spectrum and eye diagrams shown in Figs. 5(a)–(c).

If a breakpoint occurs in the fibres amongst each SBOADM (e.g. between the SBOADM2 and SBOADM3 as shown in Fig. 6), then the blocked network connection can be immediately recovered by turning the 2 $\times$ 2 OS in the RN from parallel to crossing status. In this case, the downstream optical signals in the RN will be routed to output port 2 of the 2 $\times$ 2 OS and then split to two copies by a 1 $\times$ 2 optical splitter. One copy goes into the annular main network in the clockwise direction (illustrated as downlink1) after returning to the input port 2 of the 2 $\times$ 2 OS. The other one directly goes into the annular main network in the counter-clockwise direction (illustrated as downlink2) after passing through the optical splitter. The two downstream signals will sequentially pass through each SBOADM and finally be cut off at the network breakpoint. When each dedicated optical signal is dropped to ONUs in the downlink2, it will firstly pass through the cross-status 2 $\times$ 2 OS and be directed to the OST instead of the receiver circuit inside the ONU. Subsequently, the

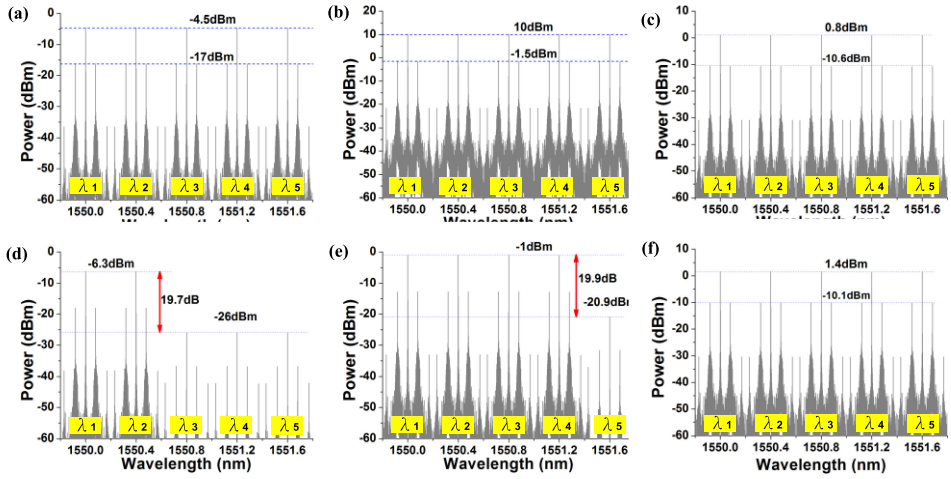

Fig. 7. Spectra measured at observation points (A)–(F) in the system shown in Fig. 6.

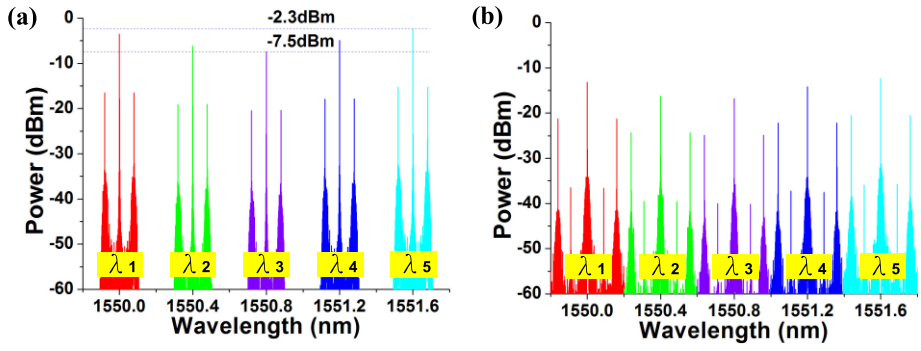

Fig. 8. (a) Overlapped spectra of the downstream optical signals dropped by each SBOADM under breakpoint occurrence. (b) Overlapped spectra of the detected upstream signals out from each ONU under breakpoint occurrence.

OST can output an electrical pulse to change the 2 $\times$ 2 SW from cross to parallel status, and then the downstream signal can be redirected to the ONU transceiver circuit.

Fig. 7 (a) to (f) are the spectra measured at observation points (A) to (F) in the system shown in Fig. 6. Figs. 7(a) and (b) respectively show identical results with that in Figs. 3(a) and (b) due to their similar passages. However, the signal power levels of the central carrier wave and side bands shown in Fig. 7(c) are roughly 3.6 and 3.4 dB lower than those in Fig. 3(c), respectively. The additional attenuation is caused by the 1 $\times$ 2 optical splitter and OS inside the RN during activation of self-recovery function. Similarly, the optical spectrum shown in Fig. 7 (f) is similar to the results in Fig. 7(c) but 0.6 dB large when the downstream signal is transmitted along the downlink2. This phenomenon is due to the passage of the optical signals in the downlink2 only in the SW inside the RN once instead of two times. When these downstream signals pass through the SBOADM5 and the SBOADM4 and SBOADM3, the central carrier power of each passed optical signal is roughly -1 and -6.3 dBm as presented in Figs. 7 (e) and (d), respectively. The power deviation between the passed and dropped optical signals is roughly 19.7–19.9 dB.

Figure 8(a) shows the overlapped spectra of the downstream optical signals dropped by each SBOADM under breakpoint occurrence. Compared with the results shown in Fig. 3(a), the power deviation amongst each signal is small and the average power levels are large. When the central

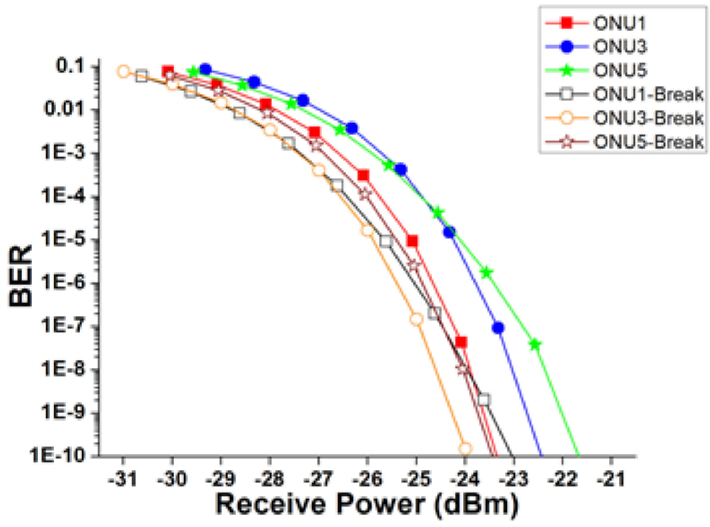

Fig. 9. Error rate of downlink signal under the system structure.

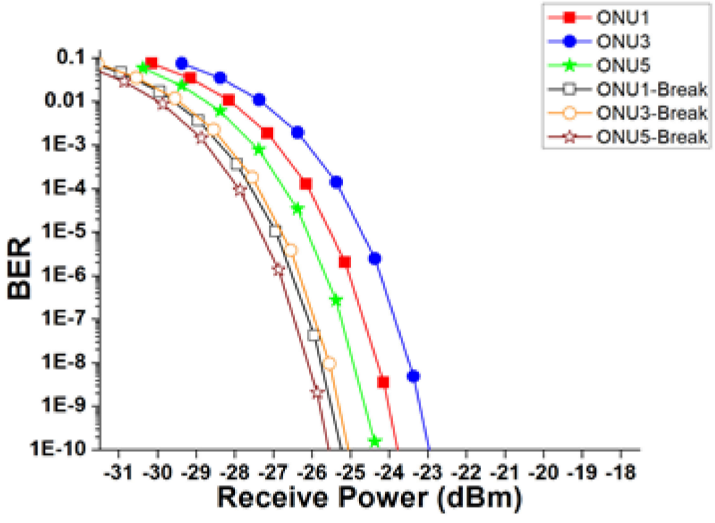

Fig. 10. Error rate of uplink signal under the system structure.

carrier wave of each dropped signal is reused to transmit the upstream signals, the spectra of the detected upstream signals from each ONU are overlapped and presented in Fig. 8(b). Compared with the results shown in Fig. 3(d), the power levels of the $\lambda 1$, $\lambda 2$ and $\lambda 3$ are roughly identical, but the $\lambda 4$ and $\lambda 5$ are enlarged due to the reset signal routing pathways.

The relative bit error rate (BER) performance for the downstream and upstream transmissions under normal and self-recovery conditions is shown in Figs. 9 and 10, respectively. Under normal situations, the impact of non-linear effect is evident during data transmissions because the overall power level is larger than that in the self-recovery condition. Therefore, the error-free transmission condition (BER $<$ 10e-9) can only be achieved at receiver power approximately -21.7 dBm under normal situations. By contrast, the value is reduced to approximately -22.2 dBm under the activation of the self-recovery function upon the occurrence of a network breakpoint because the optical power transmitted amongst SBOADMs is lower than that under normal situations. The CO can utilise suitable optical bandpass filters for the uplink transmissions to separate each optical

signal, and the average power levels of the upstream signals are initially substantially lower than those in the downstream direction. The induced non-linear effect in the upstream direction is less than that in the downstream direction. Consequently, the largest optical power level to achieve error-free transmission in the upstream direction is further reduced to roughly −23 dBm under normal or self-recovery situations. The signal of 3 Gbps/ 20 GHz is mainly utilized to verify the ability of achieving self-recovery function in the proposed architecture. A higher transmission rate, such as 400 Gbps PAM signal, is possible to be achieved by enlarging the Bragg wavelength range of the FBGs inside the SBOADMs. These results demonstrate that the proposed transport system can provide identical or improved transmission performance during breakpoint occurrence.

4. Conclusion

A full-duplex self-recovery optical fibre transport system based on a passive SBOADM is proposed in this study. The system does not need complex optical multiplexers/de-multiplexers or massive OSs to achieve full-duplex bidirectional transmission. This feature ensures the suitability of the system for the optical fibre access network based on hardware cost, operability and complexity. Moreover, the proposed transport system can achieve the self-recovery function during a fibre link failure without utilising backup fibre links during fibre link failure. The simulation results showed that a set of SBOADM only causes a power loss of approximately 2.4 dBm for passed signals. Assuming the receiving sensitivity of −22 dBm at the ONU end as the baseline, no optical amplifier is required during data transmission amongst CO and ONUs. Furthermore, PDM, frequency up-conversion and wavelength reuse techniques are employed to construct a colourless ONU to reduce the construction cost for each ONU and improve the usage efficiency of each optical channel. Therefore, the proposed transport system demonstrates remarkable flexibility and convenience in expandability and self-recovery.

References

[1] Y. J. Cheng, B T. Chen, C. P. Wu, and Y. Y. Lee, "Design of optical tunnel switching networks for big data applications," *Appl. Sci.*, vol. 10, no. 6, 2020, Art. no. 2098.

[2] Z. Wan, Z. Yu, L. Shu, Y. Zhao, H. Zhang, and K. Xu, "Intelligent optical performance monitor using multi-task learning based artificial neural network," *Opt. Express*, vol. 27, no. 8, pp. 11281–11291, 2019.

[3] J. Deng, H. Wu, R. Shan, Y. Fu, X. Liu, and P. Wang, "NPFONoC: A low-loss, non-blocking, scalable passive optical interconnect network-on-chip architecture," in *Proc. Asia-Pacific Signal Inf. Process. Assoc. Annu. Summit Conf.*, 2019, pp. 1443–1448.

[4] C. Xia *et al.*, "Time-division-multiplexed few-mode passive optical network," *Opt. Express*, vol. 23, no. 2, pp. 1151–1158, 2015.

[5] S. W. Wong, S. H. Yen, P. Afshar, S. Yamashita, and L. G. Kazovsky, "Demonstration of energy conserving TDM-PON with sleep mode ONU using fast clock recovery circuit," in *Proc. Opt. Fiber Commun. Conf.*, 2010, Paper OThW7.

[6] C. H. Yeh, C. W. Chow, C. H. Wang, F. Y. Shih, Y. F. Wu, and S. Chi, "Using four wavelength-multiplexed self-seeding Fabry-Perot lasers for 10 Gbps upstream traffic in TDM-PON," *Opt. Express*, vol. 16, no. 23, pp. 18857–18862, 2008.

[7] Y. Ma *et al.*, "Demonstration of CPRI over self-seeded WDM-PON in commercial LTE environment," in *Proc. Opt. Fiber Commun. Conf.*, 2015, Paper M2J.6.

[8] B. Schrenk *et al.*, "Passive ROADM flexibility in optical access with spectral and spatial reconfigurability," *IEEE J. Sel. Areas Commun.*, vol. 33, no. 12, pp. 2837–2846, Dec. 2015.

[9] C. Bock and J. Prat, "WDM/TDM PON experiments using the AWG free spectral range periodicity to transmit unicast and multicast data," *Opt. Express*, vol. 13, no. 8, pp. 2887–2891, 2005.

[10] S. Kimura, "10-Gbit/s TDM-PON and over-40-Gbit/S Wdm/Tdm-Pon systems with OPEX-effective burst-mode technologies," in *Proc. Opt. Fiber Commun. Conf.*, 2009, Paper OWH6.

[11] K. P. Kaur, R. Randhawa, and R. S. Kaler, "Performance analysis of WDM-PON architecture using different receiver filters," *Optik - Int. J. Light Electron Opt.*, vol. 125, no. 17, pp. 4742–4744, 2014.

[12] H. Nakamura, S. Tamaki, K. Hara, S. Kimura, and H. Hadama, "40Gbit/s λ-tunable Stacked-WDM/TDM-PON using dynamic wavelength and bandwidth allocation," in *Proc. Opt. Fiber Commun. Conf.*, 2011, Paper OThT4.

[13] J. J. O. Pires, "Constraints on the design of 2-fiber bi-directional WDM rings with optical multiplexer section protection," in *Proc. Adv. Semicond. Lasers Appl./Ultraviolet Blue Lasers Appl./Ultralong Haul DWDM Transmiss. Netw./WDM Components*, 2001, Paper MC3.2.

[14] S. Dewra and R. S. Kaler, "Performance evaluation of an optical network based on optical cross add drop multiplexer," *J. Opt. Technol.*, vol. 80, no. 8, pp. 502–505, 2013.

[15] Z. Wang, C. Lin, and C. K. Chan, "Demonstration of a single-fiber self-healing CWDM metro access ring network with unidirectional OADM," *IEEE Photon. Technol. Lett.*, vol. 18, no. 1, pp. 163–165, Jan. 2006.

[16] P. Chanclou, L. A. Neto, G. Simon, A. E. Ankouri, S. Barthomeuf, and F. Saliou, "FTTH and 5G xhaul synergies for the present and future," in *Proc. 21st Int. Conf. Transparent Opt. Netw.*, 2019, Paper We.D2.2.
[17] F. Bao *et al.*, "DSP-free single-wavelength 100 Gbps SDM-PON with increased splitting ratio using 10G-class DML," *Opt. Express*, vol. 27, no. 23, pp. 33915–33924, 2019.
[18] D. V. Veen, "Transceiver technologies for next-generation PON," in *Proc. Opt. Fiber Commun. Conf.*, 2020, Paper W1E.2.
[19] N. N. Cikan and M. Aksoy, "A review of self-seeded RSOA based on WDM PON," *Can. J. Elect. Comput. Eng.*, vol. 42, no. 1, pp. 2–9, 2019.
[20] Z. Zhang *et al.*, "Optical- and electrical-domain compensation techniques for next-generation passive optical networks," *IEEE Commun. Mag.*, vol. 57, no. 4, pp. 144–150, Apr. 2019.
[21] M. Šprem and D. Babić, "Wavelength reuse WDM-PON using RSOA and modulation averaging," *Opt. Commun.*, vol. 451, no. 15, pp. 1–5, 2019.
[22] D. R. Celinoa, U. R. Duarteb, and M. A. Romero, "Improved self-seeding and carrier remodulation performance for WDM-PON by means of double RSOA erasure," *Opt. Commun.*, vol. 459, 2020, Art. no. 125018.
[23] C. H. Chang, D. Y. Lu, and W. H. Lin, "All-passive optical fiber sensor network with self-healing functionality," *IEEE Photon. J.*, vol. 10, no. 4, Aug. 2018, Art. no. 7203310.
[24] Z. Jia, M. Xu, J. Zhang, H. Zhang, L. Campos, and C. Knittle, "Demonstration of low-latency coherent optical connectivity for consolidated inter-hub ring architecture," in *Proc. Opt. Fiber Commun. Conf.*, 2020, Paper Th3A.2.
[25] L. Xu, N. Chi, L. K. Oxenløwe, J. Mørk, S. Yu, and P. Jeppesen, "A new orthogonal labeling scheme based on a 40-Gb/s DPSK payload and a 2.5-Gb/s PolSK label," *IEEE Photon. Technol. Lett.*, vol. 17, no. 12, pp. 2772–2774, Dec. 2005.